EXAMINATION OF INTEGRAL SPECTRA OF INDIUM BROMIDE DIELECTRIC FUNCTION

M.I. Kolinko[1], O.V. Bovgyra[1], A.H. Nevidomskyy[1],
I. Kityk[2], P. Bragiel[2], M. Piasecki[2]

[1]Physics Faculty, Ivan Franko National University of Lviv, Ukraine
[2]Pedagogical University at Czestochowa, Poland

INTRODUCTION

Indium bromide single crystals that have been synthesized comparatively lately, as well as other representatives of the family of the third group metals monohalides are being intensively investigated from the point of view of their possible use as functional materials in the infrared region for laser technology and fiber optics. Recently they have found industrial application as materials for producing photodetectors used in scintillation spectroscopy of nuclear radiation as well [1]. Although the reflection, absorption, and emission spectra are usually studied in a comparatively narrow energy interval near the fundamental absorption edge, the results attest to a strong dichroism due to the anisotropic crystalline ordering [2-5]. The spectra of this compound, like the spectra of alkali-halide crystals, have a pronounced excitonic character. It has been found, however, that the principal structures of the spectra are markedly different in structure, character, and temperature behavior from the spectra of the isostructural and isoelectronic single crystals a-TlI and InI.

However the properties of layered halogenides of metals of the third group can hardly be explained without information about their energy structure and contribution of ion terms into the formation of the optical spectra.

Since no results of calculations of the energy-band diagram of indium bromide have yet been published, it is reasonable to use an alternative way of studying the electronic structure of this compound, viz., to determine the spectral distribution of the optical constants employing radiation in the energy range under study and using different polarizations of the probe radiation over a wide temperature interval.

This paper is devoted to the determination of the entire spectrum of optical transitions of InBr single crystals as well as their parameters. The dielectric functions $\varepsilon_1(E)$ and $\varepsilon_2(E)$ calculated by means of the Kramers—Kronig method based on the low-temperature experimental reflection spectra, are determined by all the set of oscillators. Such spectra contain little information, thus it is necessary to decompose the integral curves of real and imaginary parts of dielectric function into separate components, which are related to the groups of interband

transitions with almost the same parameters in the region of certain points in the Brillouin zone.
The bands overlap so strongly in the crystals with complicated energy spectrum, as in InBr, that the direct determination of the band parameters is impossible. In this case different methods of decomposition of integral curves (usually the imaginary part of dielectric function ε_2) into constituents are used. The shape of individual constituent is assumed to be of Lorentz or Gaussian type.
We have used the unambiguous method of decomposing the integral curves of dielectric function ε_2 into the elementary components, which is based on the consideration of the spectrum of ε_2 as a function of ε_1 by means of Argand diagram technique. This method assures not only the larger reliability of the constituents obtained in comparison with purely mathematical methods, but also permits to reveal additional bands, which are not visible in the optical spectra.
The use of the known data on the optical properties and band diagrams of the isostructural III-VII compounds makes it possible to do an initial identification of the principal structures of the spectra both from a topological and from polarization and crystal-chemical points of view.

CALCULATION TECHNIQUE

The most complete and visual information about the peculiarities and parameters of the electronic spectra are contained in the complex of fundamental optical functions, which were determined by us using the technique that had been approved not once [6-8]. The extrapolation into the energy region that lies beyond measurements was carried out by power-law functions, with parameters found by solving determinant boundary conditions in the transparency region where phase is known to be equal to zero $\Theta(E)\equiv 0$.
Among the optical constants, the real ε_1 and imaginary ε_2 parts of the dielectric function have a special status. This is because their spectra, like those of the reflectivity, can be measured over a wider energy interval than can the other optical functions, such as, e.g, the refractive index n or the absorption coefficient κ. In addition, the energies of the reflection peaks and of the imaginary part of the dielectric function are commonly associated with the energies of the interband or excitonic transitions.
However, experimental reflection curve and the optical functions that were calculated on its basis result in the integral curve as a sum of contributions from all transitions over all Brillouin zone. Because of the large half-width of the transition bands and their strong overlapping most of them cannot be structurally observed in the integral spectra of R and ε_2. We have developed the unambiguous method of dividing spectral curve ε_2 into elementary components and determining their

basic parameters such as: maximum energies E_i, half-widths H_i, as well as oscillator strengths f_i, obtained by applying Argand diagram technique.

Division of integral spectrum ε_2 into individual components was made in the well-known from the electron theory representation of the dielectric constant as a sum of symmetric Lorentz oscillators:

$$\varepsilon_1(E) - 1 = \sum_{i=1}^{N} \frac{A_i(E_i^2 - E^2)}{(E_i^2 - E^2)^2 + H_i^2 E^2};$$

$$\varepsilon_2(E) = \sum_{i=1}^{N} \frac{A_i H_i E_i}{(E_i^2 - E^2)^2 + H_i^2 E^2},$$

where E_i is energy value, H_i – half-width, N – number of oscillators, and the value of A_i is equal to

$$A_i = \frac{4\pi n_0 e^2 \hbar^2}{m} f_i,$$

the quantity f_i is called the oscillator strength.

Argand diagram technique is based on the fact that for one isolated symmetric Lorentz oscillator the dependence $\varepsilon_2 = f(\varepsilon_1)$ has a form of circle. The coordinates of its center and the radius of the circle determine the three parameters of the oscillator. Generally, the overlapping of the set of large number of bands the Argand curves have rather complicated shape. However, there are usually several regions on them that can be well extrapolated by semi-circles, which correspond to the isolated oscillators that are almost not distorted by neighboring interband transitions. From the integral Argand diagram we subtracted the partial contributions of such oscillators and then again marked out the parts, which could be well described by semi-circles. Such a procedure was repeated until there appeared the well-expressed semi-circles on the remainders of Argand curves.

The set of the effective Lorentz oscillators that were determined in such a way is unambiguous. The band of each component can be further divided into a number of subbands, that is, every effective oscillator combines the transitions with close energy values which can be however, of different nature.

Of course, the Argand diagram technique of dividing the integral spectra ε_2 and ε_1 into components is considerably simplified and is a kind of the zero approach for more perfect schemes of solving this problem. The theoretical analysis of individual bands might then show that each of them should be further divided into several components.

EXPERIMENTAL PROCEDURE

Indium bromide was obtained using chemical reaction between metallic indium and liquid bromine in vacuum with excess of indium for perverting formation of $InBr_3$. The single crystals were grown from the melt by the Bridgman method after repeated purification; they were easily cleaved in one definite direction, and the mirror surfaces or me samples did not require additional treatment. X-ray monitoring, which confirmed the space group of the InBr crystals (*CmCm*), showed that the cleavage plane was perpendicular to the b axis.
As a source of synchrotron radiation the accelerator with energy 600 MeV had been used. The operating pressure was within $1.3 \cdot 10^{-6}$ Pa. The incident and reflected radiation were analysed with sodium salicylate. As a monochromator we used vacuum spectrometer Seya Numioka. Measurements were carried out for three incidence angles: 8°, 12°, 16° and the data being obtained were analysed using specially constructed computer code. Spectral resolution was 0.7 nm/mm. The absolute values of reflectivity had been obtained using germanium single crystal. The spectra were recorded at liquid-helium temperature.

RESULTS AND DISCUSSION

The initial data for calculations of the fundamental optical functions were the experimental measurements of low-temperature polarization-dependent reflection spectra that are shown in Fig. 1.
The plastic properties of this compound caused the difficulties in obtaining sample surfaces of high quality to be used in investigations of Ellb polarization. In general the spectra in Fig. 1 can be partitioned into four regions that differ in the character and behavior of the reflectivity curve: up to ≈4.7 eV, from 4.7 up to 7.5 eV, from 7.5 up to 16 eV and higher than 16 eV. Let's note that in the entire energy region the reflectivity for Ellc polarization is larger than that for Ella polarization except for two narrow intervals 4.7–6 eV and 14–15 eV.
If the layered compounds show the dichroism of optical properties between the directions which lie in the wafer plane and that direction which is perpendicular to this plane, then in the case of indium bromide the anisotropic nature of the crystal exhibit itself in the plane of the layer as well, as can be seen from Fig. 1.

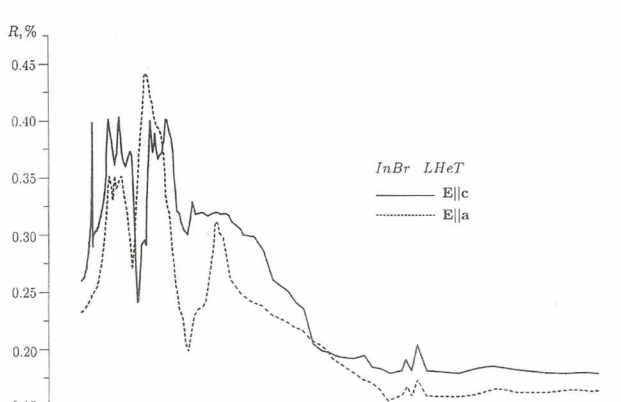

Fig. 1. Polarization-dependent reflection spectra of indium bromide single crystals

To determine the correspondence between the measured spectrum and the interband energy intervals, we calculated the real ε_1 and imaginary ε_2 parts of the dielectric function, which are shown in Fig. 2; they establish a direct connection between the microscopic and macroscopic characteristics of the crystals. The extrema of ε_2 correlate with the maxima of the reflectivity without any noticeable shift. However, between the spectra of the functions obtained for different polarizations of the radiation a pronounced dichroism is observed across nearly the entire energy interval of the radiation, and not only near the fundamental absorption edge. In addition, we note that for both polarizations one can discern more than ten oscillators in the region below 15 eV, whereas in the high-energy region the peaks in the spectra ot the dielectric function are very weakly manifested.

By using the Argand diagram procedure we have carried out separation of the ε_2 spectra of InBr into the elementary components for different polarizations, which are shown in Fig. 3. The parameters of these components, such as the maximum energies, half-width, and the oscillator strengths, were determined as well. For the energy region of 2-28 eV twenty eight components of the ε_2 spectrum were found out for the Ella polarization and thirty five components for the Ellc polarization (table 1).

The oscillator strength f_i is often being averaged over the total number of valence electrons. In this case f_i is proportional to the area of the band in the integral $\varepsilon_2(E)$ spectrum, but if the spectrum of the effective number of valence electrons $n_{eff}(E)$ is available then it is more correct to use these data in calculations of f_i.

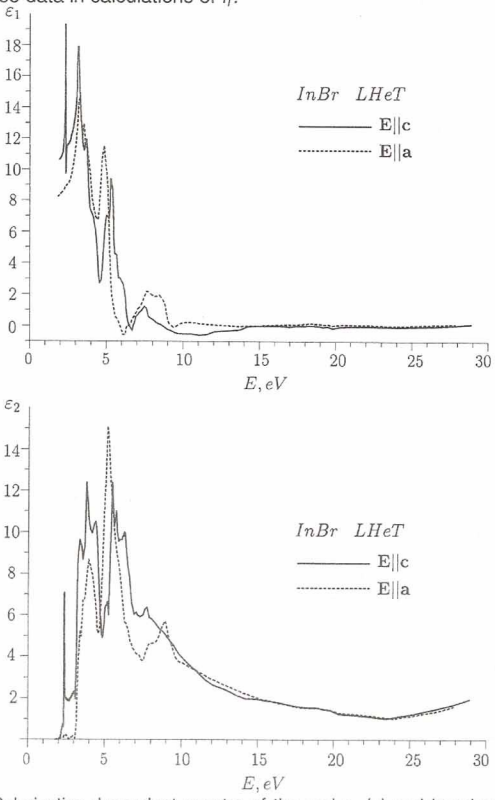

Fig. 2. Polarization-dependent spectra of the real ε_1 (a) and imaginary ε_2 (b) parts of the dielectric function of InBr single crystals

The comparison of our results with the data of theoretical calculations of energy band structure of isostructural and isoelectronic compounds

TII and InI enabled us to make the initial identification of the main peaks in the spectra of dielectric function.

The unambiguous determination of the nature of the components of ε_2 spectrum is a difficult task. As yet there is no common theory of optical properties, which would combine the models of direct interband gaps and the model of metastable excitons [12]. The conventional qualitative model says that the most intensive interband and correspondingly, the exciton transitions, should be observed between those pairs of bands, which are parallel to each other in the certain subvolume of the Brillouin zone.

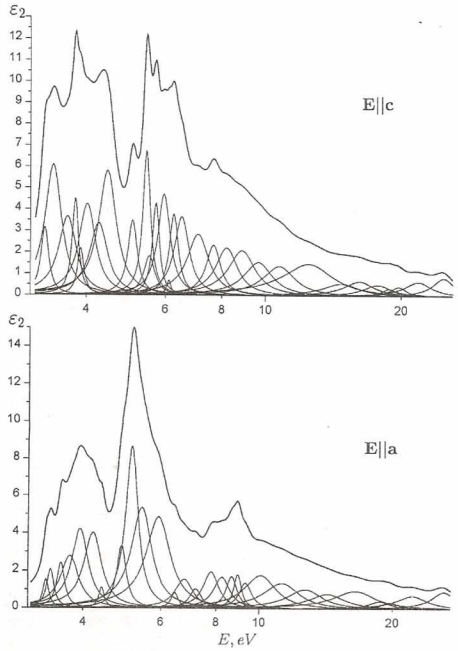

Fig.3. Integral spectra of ε_2 of InBr for different polarizations and their decomposition into individual components. The logarithmic energy scale is used

The other polar model based on the metastable excitons is considered to be rather perspective. The maxima of the ε_2 spectrum can be

considerably easier described within the latter model, but the calculations of the metastable excitons do not, to our knowledge, exist as yet. That is why the nature of optical spectra is being discussed here within the model of interband transitions.

Band diagrams for InI [9] and TlI [10,11] that were studied enable us to assert that valence complex of these compounds is structured and can be presented with the following sequence of bunches of bands: 2-4-2-2 (counting from the top of the valence band in the order of increase of the bonding energy).

Table 1. Parameters E_i, H_i, f_i of oscillators (O_i) of InBr

	Ellc			*Ella*		
O_i	E_i, eV	H_i, eV	f_i	E_i, eV	H_i, eV	f_i
O_1	2.34	0.026	1.36	3.30	0.12	0.98
O_2	2.50	0.24	1.18	3.37	0.15	1.01
O_3	2.65	0.22	0.76	3.56	0.17	0.80
O_4	2.84	0.21	0.82	3.94	0.42	0.97
O_5	3.22	0.14	0.88	3.74	0.43	0.98
O_6	3.31	0.22	0.91	4.21	0.47	0.68
O_7	3.43	0.24	0.55	4.41	0.15	0.05
O_8	3.62	0.35	0.56	4.89	0.29	0.23
O_9	3.77	0.15	0.20	5.15	0.40	0.52
O_{10}	3.88	0.16	0.08	5.43	0.71	0.40
O_{11}	4.01	0.44	0.37	5.94	0.93	0.39
O_{12}	4.26	0.55	0.28	6.45	0.30	0.02
O_{13}	4.45	0.52	0.41	6.79	0.77	0.10
O_{14}	5.06	0.27	0.12	7.20	0.54	0.05
O_{15}	5.44	0.26	0.19	7.80	0.76	0.13
O_{16}	5.52	0.39	0.07	8.25	0.85	0.13
O_{17}	5.71	0.25	0.10	8.68	0.60	0.09
O_{18}	5.95	0.46	0.19	8.96	0.44	0.07
O_{19}	6.11	0.16	0.01	9.33	0.74	0.09
O_{20}	6.26	0.34	0.10	10.14	2.02	0.31
O_{21}	6.52	0.59	0.16	11.35	2.55	0.31
O_{22}	7.10	0.96	0.19	12.80	2.89	0.28
O_{23}	7.67	0.68	0.11	14.38	3.35	0.26
O_{24}	8.21	1.13	0.17	16.65	4.50	0.47
O_{25}	8.90	1.50	0.21	18.77	2.58	0.12
O_{26}	9.68	1.75	0.18	19.80	2.22	0.09
O_{27}	10.80	2.15	0.21	22.29	4.45	0.41
O_{28}	12.64	3.99	0.45	26.15	3.98	0.54
O_{29}	14.87	3.35	0.16	–	–	–
O_{30}	16.25	3.10	0.18	–	–	–
O_{31}	17.80	3.03	0.16	–	–	–
O_{32}	18.83	1.67	0.06	–	–	–
O_{33}	19.77	1.78	0.08	–	–	–
O_{34}	21.94	3.72	0.27	–	–	–
O_{35}	24.88	3.22	0.33	–	–	–

On the basis of these diagrams and selection rules (table 2) for interband transitions in different points and lines in the Brillouin zone it is possible to determine the approximate sequence of transitions near the edge of fundamental absorption.

We do not provide in the Table 2 the transitions for Γ-point since the least interband intervals in all compounds of A_3B_7 family are formed far from the center of the Brillouin zone, which is shown in Fig. 4. This characteristic peculiarity of the gaps being localized near the edges of the Brillouin zone comes out mostly from the electronic configuration of these ten-electron compounds, which includes an extra *s*-electron pair of the cation. We also exclude from the consideration *Y*-point and the whole Δ-line since the energy intervals are very wide here and they play no role in the formation of the absorption edge region.

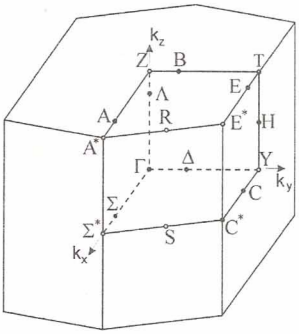

Fig.4. The Brillouin zone of base-centered orthorhombic lattice

The least direct gap in [4,10] is related to the *T* point of the Brilouin zone, however, the calculations [9,11] show that the least intervals are localized near the Σ^* point (and in the equivalent C^* point), and along the *S* and *H* lines. Besides, the transition in the *T* point cannot explain the polarization dependence of the first direct exciton, which should have been connected with this point. According to the Table 2 this transition can take place only on the lines Σ ($\Sigma_{4,v} \rightarrow \Sigma_{2,c}$) and *H* ($H_{3,v} \rightarrow H_{3,c}$).

Table 2. Allowed optical interband transitions in the high-symmetry points and lines of the Brillouin zone [9]

Points Lines	Ella	Ellb	Ellc
Z (T)	$Z_1 \rightarrow Z_2$ $Z_2 \rightarrow Z_1$	$Z_1 \rightarrow Z_1$ $Z_2 \rightarrow Z_2$	$Z_1 \rightarrow Z_1$ $Z_2 \rightarrow Z_2$
S	$S_1^+ \rightarrow S_2^-$ $S_1^- \rightarrow S_2^+$ $S_2^+ \rightarrow S_1^-$ $S_2^- \rightarrow S_1^+$	$S_1^+ \rightarrow S_2^-$ $S_1^- \rightarrow S_2^+$ $S_2^+ \rightarrow S_1^-$ $S_2^- \rightarrow S_1^+$	$S_1^+ \rightarrow S_1^-$ $S_1^- \rightarrow S_1^+$ $S_2^+ \rightarrow S_2^-$ $S_2^- \rightarrow S_2^+$
Σ	$\Sigma_1 \rightarrow \Sigma_1$ $\Sigma_2 \rightarrow \Sigma_2$ $\Sigma_3 \rightarrow \Sigma_3$ $\Sigma_4 \rightarrow \Sigma_4$	$\Sigma_1 \rightarrow \Sigma_4$ $\Sigma_2 \rightarrow \Sigma_3$ $\Sigma_3 \rightarrow \Sigma_2$ $\Sigma_4 \rightarrow \Sigma_1$	$\Sigma_1 \rightarrow \Sigma_3$ $\Sigma_2 \rightarrow \Sigma_4$ $\Sigma_3 \rightarrow \Sigma_1$ $\Sigma_4 \rightarrow \Sigma_2$
H (Λ)	$H_1 \rightarrow H_4$ $H_2 \rightarrow H_3$ $H_3 \rightarrow H_2$ $H_4 \rightarrow H_1$	$H_1 \rightarrow H_3$ $H_2 \rightarrow H_4$ $H_3 \rightarrow H_1$ $H_4 \rightarrow H_2$	$H_1 \rightarrow H_1$ $H_2 \rightarrow H_2$ $H_3 \rightarrow H_3$ $H_4 \rightarrow H_4$

The indirect transition in [4] is considered to be connected with the dipole transition in the T-point and the successive scattering of a hole or an electron down to the point S with help of the momentum-conserving phonons. However, this scheme is impossible, since the gap in the T point is larger than that in the S point in these compounds. Moreover, the conduction band in the T point is localized higher than in the S point, while the valence band is lower.

According to the Table 2 and the results [9,11] other scheme is more probable, in which such a transition will take place either on the line between two equivalent points Σ^* and C^* (where the S point is also situated) or in the T point with successive electron scattering towards the Σ or H lines direction.

It is important to stress that the main structures of the reflection spectra will be determined by the transitions in the region of almost parallel bands which lie between these Σ^* and C^* points.

The intensive structures in the energy region up to 4.7 eV are formed by the transitions from the two highest valence bands, which come from 4pBr and 5sIn orbitals. The next region from 4.7 up to 7.5 eV is caused by the transitions from the four valence bands, which are formed by p_x-, p_y- and p_z- bromine electrons. The minimum of ε_2(E) near the energy value of 7.5 eV marks the end of transitions from the next two bands of a mixed origin, which are separated from the previous ones by the slight energy interval.

The structure of the spectrum in the region between 7.5 and 16 eV is due to the transitions from the mentioned eight bands to higher

conduction bands. After 16 eV the dychroism motive ceases to be dominating in the optical spectra, i.e. after the transitions from the upper, valence bands have been scooped out, while the deep levels are less effected by the influence of anisotropic crystalline field.
The further results for the ε_2 spectrum obtained on the basis of theoretical electron-band calculations can enable us to carry out the rigorous analysis of the oscillators of the optical transitions taking into account the selection rules for different light polarizations.

SUMMARY AND CONCLUSIONS

We have accomplished the decomposition of integral curves of dielectric functions of indium bromide layered single crystals into individual components using the Argand diagram technique. Three basic parameters of each component (the energies of the maximum, the halfwidth, the oscillator force) were obtained.
The decomposition was carried out using the well known from the electronic theory representation of the dielectric function as a sum of contributions of symmetric Lorentz oscillators. The set of such effective oscillators that we have determined for InBr appears to be minimal. Each component assembles the transitions that are close in their energies, however they may be of a different origin.
A primary interpretation of the principal structures of the spectra is offered on the basis of the known band-energy structure calculations of isostructural and isoelectronic group-III metal halides.
The complex of fundamental optical functions obtained, as well as the components of the spectrum of dielectric function supplement the experimental information in a very wide and deep fashion.
This provides a principally new basis for accurate theoretical calculations of the subtle peculiarities of the electronic structure of strongly anisotropic compounds, in particular, of indium bromide.

REFERENCES

K.S. Shah, L.P. Moy, J. Zhang, S. Medrick, F. Olschner and M.R. Squillante, SPIE Proceedings **1734**, 161, (1992).
F. Levy and E. Mooser, Helv. Phys. Acta **45**, 69 (1972).
M.I. Gelten, P. Hoenderdos, J.Phys. Chem. Solids **35**, 653 (1974).
M. Yoshida, N. Ohno, H. Watanabe, K. Nakamura, Y. Nakai, J. Phys. Soc. Japan **53**, 408 (1984).
A. Borghesi, G. Guizzetti, L. Nosenzo, E. Reguzzoni, A. Stella, F. Levy, Solid State Commun. **48**, 345 (1983).
V.V. Sobolev, S.A. Alekseeva and V.I. Donetskikh. Calculations of Optical Functions of Semiconductors from the Kramers–Kronig Relations [in Russian], Shtiintsa, Kishinev (1976).
K. Jezierski, J. Phys. C: Solid State Phys. **19**, 2103 (1986).
M.I. Kolinko, O.V. Bovgyra, and M. Piasecki, Low Temp. Phys. **27**, 153 (2001).
M.I. Kolinko, J. Phys.: Condens. Matter **6**, 183 (1994).
J.P. Van Dyke, G.A.. Samara, Phys. Rev. B **11**, 4935 (1975).
M.I. Kolinko, I.V. Kityk, A.S. Krochuk, J. Phys. Chem. Solids **53**, 1315 (1992).
V.V. Sobolev, V.V. Nemoshkalenko. The Methods of Computational Physics in Solid State Theory. Electronic Structure of Semiconductors. [in Russian], Naukova Dumka, Kiev (1988).